

Correlation of cyclic preloading with the liquefaction resistance

T. Wichtmann¹⁾, A. Niemunis, Th. Triantafyllidis, M. Poblete

Institute of Soil Mechanics and Foundation Engineering, Ruhr-University Bochum, Universitätsstraße 150, 44801 Bochum, Germany

Abstract

The compactivity of sand due to cyclic loading with a high number ($N > 10^3$) of small cycles ($\epsilon^{\text{ampl}} \leq 10^{-3}$) cannot be described by void ratio and stress alone. It depends strongly on the soil fabric usually described as "cyclic preloading". The cyclic preloading cannot be measured directly in situ but correlates well with the liquefaction resistance. This paper demonstrates this correlation on the basis of laboratory tests. Practical applications can be derived from this work.

Key words: Cyclic preloading; liquefaction resistance; correlation; cyclic undrained triaxial tests; sand

1 Introduction

Under drained conditions a cyclic loading leads to an accumulation of settlements. Even small amplitudes can significantly contribute if the number of cycles is high ($N > 10^3$). The settlements (and excess pore water pressures in the undrained case) may endanger the serviceability of foundations, e.g. of transportation structures, tanks, watergates, wind power plants.

Our aim is the numerical prediction of the residual settlements under high-cyclic loading. A special accumulation model was developed for this purpose (Niemunis et al. [1]). It is based on numerous cyclic laboratory tests performed on freshly pluviated specimens (Wichtmann et al. [2,3,4]).

These tests show, that a cyclic preloading significantly affects the accumulation rate, Fig. 1. Three cyclic triaxial tests at an identical stress and void ratio (in Fig. 1 marked by the horizontal line at $e = 0.629$) have different densification rates $\dot{e} = \partial e / \partial N$. A freshly pluviated specimen densifies much faster compared to a preloaded specimen (= after several thousand load cycles). Thus, apart of stress and void ratio the accumulation rate depends on cyclic preloading. Possible causes of cyclic preloading in situ can be a seismic activity in the past, repeated sedimentation and erosion processes, an oscillating ground water level, etc.

¹⁾Corresponding author. Tel.: + 49-234-3226080; fax: +49-234-3214150; e-mail adress: torsten.wichtmann@rub.de

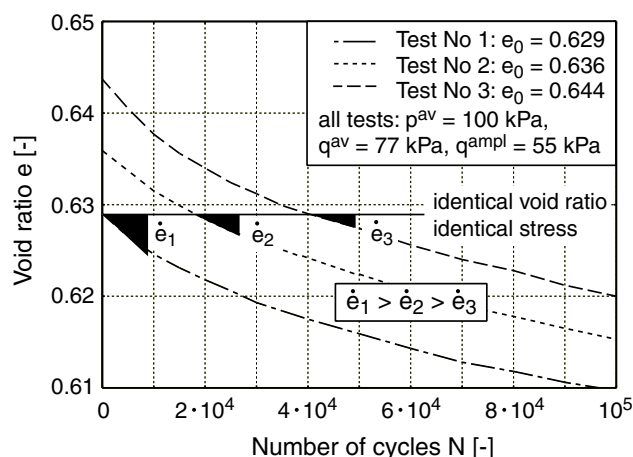


Fig. 1: Impact of a cyclic preloading on the accumulation rate $\dot{e} = \partial e / \partial N$ (drained cyclic triaxial tests)

The cyclic preloading is generally unknown in situ and no methods for its assessment are established so far. The in-situ fabric cannot be measured directly. Laboratory testing on undisturbed intact specimens of high quality (e.g. obtained by means of ground freezing, Yoshimi et al. [5], Hofmann et al. [6]) is technically difficult and expensive. It is thus necessary to develop a simple and economic method for the determination of the cyclic preloading.

We have studied various manifestations of the evolution of fabric under cyclic loading. Our first attempt

was to observe spatial fluctuations of contact forces (force chains) in an oedometer before and after cyclic loading (Humme [7]). No clear change of the offprints could be detected. Next we have studied the fluctuation of the strain field (accumulative or in a single cycle) by means of the particle image velocimetry (PIV) method, Niemunis [8]. However, the fluctuation did not significantly change during cyclic loading. We have also studied a correlation of cyclic preloading with small strain stiffness. The small strain stiffness was expected to increase with an abatement of the spatial stress fluctuations. Unfortunately, the performed resonant column tests and cyclic triaxial tests with P- and S-wave measurements did reveal that such a correlation is not clear enough for a practical application, Wichtmann and Triantafyllidis [9,10].

This paper presents the experimental evidence that cyclic preloading strongly correlates with the liquefaction resistance. A practical application of this correlation seems promising, since one can make advantage of the data from numerous studies on the liquefaction resistance in the literature, Sec. 2.

2 Literature review

The development of research on the field of pore water pressure accumulation and liquefaction due to undrained cyclic loading may be tracked in several state-of-the-art publications, e.g. Yoshimi et al. [11], Seed [12], Dobry [13], Ishihara [14], Robertson and Fear [15]. An overview of the actual standard of knowledge may be also found in Triantafyllidis (ed.) [16]. The following literature review concentrates on the effect of fabric or cyclic preloading on the liquefaction resistance and possibilities to assess the liquefaction resistance in situ.

It is well known, that varying sample preparation techniques lead to different initial soil fabrics (*inherent anisotropy*). Slightly elongated grains e.g. tend to lie with their longer axes in the horizontal plane if they are dry pluviated, whereas a random distribution of the orientations is achieved by layering and tamping of moist sand (Nemat-Nasser and Takahashi [17]). The initial fabric affects the liquefaction resistance. Ladd [18] observed that sand specimens which were prepared by moist tamping could sustain around four times more cycles to liquefaction than specimens that were dry pluviated and compacted by vibration. Similar tendencies could be conformed by the tests of Mulilis et al. [19,20]. Porcino et al. [21] reported that air pluviation leads to a significantly lower liquefaction resistance than water pluviation. Oda et al. [22] pointed out the significance of the direction of deposition compared to the polarization of cyclic loading. Specimens

that were loaded perpendicular to the direction of deposition exhibited a higher cyclic liquefaction resistance than the ones loaded parallel. Many authors found the sensitivity to liquefaction of high-quality undisturbed specimens to be significantly lower than the one of re-constituted specimens, irrespectively of the method of preparation (Mulilis et al. [19,20], Tokimatsu and Hosaka [23], Hatanaka et al. [24], Porcino et al. [21]).

Pioneer work on the effect of an undrained cyclic preloading on the liquefaction resistance was done by Finn et al. [25]. In triaxial tests they applied a cyclic undrained loading followed by a re-consolidation and a second cyclic undrained test phase. The preloading was stopped when liquefaction already occurred after the generation of a certain axial strain amplitude $\varepsilon_1^{\text{ampl}}$. Large strain amplitudes (e.g. $2\varepsilon_1^{\text{ampl}} = 5 \cdot 10^{-2}$) decreased the liquefaction resistance in the subsequent phase dramatically. If the first test phase was stopped already at relative small strain amplitudes ($2\varepsilon_1^{\text{ampl}} < 2 \cdot 10^{-3}$) the re-liquefaction resistance was higher than the resistance of a virgin specimen. Thus, small to medium strain amplitudes increase the liquefaction resistance while large amplitudes lead to a reduced undrained cyclic strength.

The effect of small cycles was also studied by Seed et al. [26], who performed shaking table tests under simple shear conditions. Packages with a small number of cycles N (smaller than N causing liquefaction) were applied in succession to the saturated sand each simulating an earthquake of low intensity. After each package the sand layer was re-consolidated. Seed et al. observed that the pore water pressure rise became slower with each succeeding package, i.e. with increasing cyclic preloading. Other experimental studies (Seed et al. [27], Teachavoransinsun et al. [28]) support the increase of the liquefaction resistance due to cyclic preloading with small amplitudes.

Ishihara and Okada [29,30] distinguished between *small prestraining* with effective stress paths that do not surpass the phase transformation (PT) line and *large prestraining* where the stress path goes beyond the PT line. Small prestraining increases the liquefaction resistance. On the other hand, if a soil was subjected e.g. to a large prestraining on the triaxial compression side, in a subsequent cyclic loading with reversing shear stresses less pore water pressure was generated on the compression side but a larger one developed on the extension side (compared to non-presheared specimens).

Suzuki and Toki [31] found a peak in the curves of the number of cycles required to cause liquefaction plotted versus the maximum shear strain during prestraining. The strain at this peak was called *threshold strain* and lay between $4 \cdot 10^{-3}$ and 10^{-2} depending on the type of preshearing (e.g. drained or undrained cycles, cycles

towards the compression or the extension side or cycles with reversing directions). Smaller prestraining amplitudes improved the liquefaction resistance while larger ones caused a reduction. The decrease of the liquefaction resistance for higher shear strains was evoked without liquifying during prestraining. Surprisingly, Suzuki and Toki did not find any difference in the liquefaction resistance for a preloading with one or with ten cycles (contrary to our tests, see Section 4).

Emery et al. [32] found a loosening of the upper part of the specimen due to liquefaction and attributed the decrease in the re-liquefaction resistance at higher strains to this non-uniformity of the specimens. However, Oda et al. [22] demonstrated, that although loose layers within a specimen affect its cyclic undrained behaviour the effects are not significant enough to explain the strong reduction of the liquefaction resistance due to large cyclic prestraining. Oda et al. supposed changes in the soil fabric to be responsible.

Although several authors studied the influence of cyclic preloading on the liquefaction resistance, no quantitative correlation has been formulated so far.

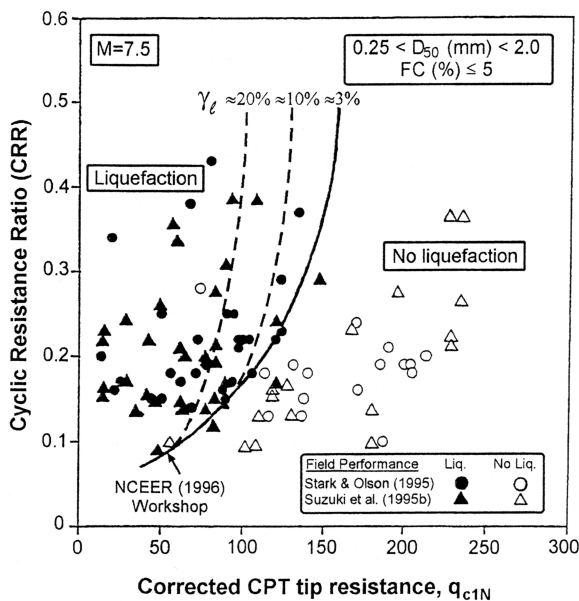


Fig. 2: Estimation of the liquefaction resistance from CPT data (Robertson and Wride [41])

The liquefaction resistance of an in-situ soil can be estimated from the penetration resistance measured in SPT soundings (Seed et al. [12,33,34]) or from the CPT tip resistance (Robertson and Campanella [35], Seed and de Alba [36], Mitchell and Tseng [37], Olsen and Koester [38], Suzuki et al. [39], Stark and Olson [40], Robertson and Fear/Wride [15,41]). Correlation diagrams as the one in Fig. 2 (Robertson and Wride [41]) are obtained from investigations whether an in-situ soil deposit has liquefied during an earthquake in the past

or not. With the estimated intensity of earthquake shaking and SPT or CPT data before the earthquake a threshold line can be found separating the cyclic stress ratios $CSR = \tau^{amp}/p_c$ (shear stress amplitude τ^{amp} , effective mean pressure p_c) that lead to liquefaction from those which do not. Similar threshold curves can be obtained from laboratory tests on undisturbed specimens (Ishihara [14]).

In Fig. 3a (for SPT) and Fig. 3b (for CPT) Ishihara [14] collected threshold lines from several authors and standard codes at practice. The lines scatter in dependence on the grain size distribution and the silt content. In order to use the diagrams in Figs. 2 and 3 the measured SPT blow number N or CPT tip resistance q_c has to be normalized by the overburden pressure and possibly corrected by the driving energy. The influence of the fines content can also be considered by using correction factors as proposed by Robertson and Wride [41]. The threshold curves in the diagrams in Figs. 2 and 3 refer to an earthquake of the magnitude 7.5 with an equivalent number of cycles $N_{eq} = 15$, Robertson and Wride [41].

3 Objective of the experiments, test device, specimen preparation and tested material

The aim of the current experimental study was the formulation of a correlation between the intensity of cyclic preloading (*small prestraining* in the terminology of Ishihara and Okada [29,30]) and the liquefaction resistance. This correlation was established on the basis of laboratory tests. In the triaxial tests the specimens were first subject to a drained cyclic preloading with a definite number of cycles and a given stress amplitude. Afterwards the drainage was closed and the cyclic undrained strength was determined. Four different cyclic preloading histories were tested.

A scheme of the used triaxial device is presented in Fig. 4. The axial load was applied by the upper cross-beam of a freely programmable load press driven by an electrical servo motor. In the cyclic tests the axial load was varied between specified minimum and maximum forces driving with a constant strain rate. Due to the changes of the specimen stiffness during undrained cyclic loading this testing procedure lead to some variations in the loading frequency during the test ($f = 0.01$ Hz was intended), especially around the onset of liquefaction.

The axial load was measured at a load transducer inside the pressure cell below the specimen base plate. A displacement transducer fixed to the load piston was used to monitor vertical deformations. Volume changes during the consolidation and the drained cyclic test phases were determined from the squeezed out pore water using a differential pressure transducer. Cell pres-

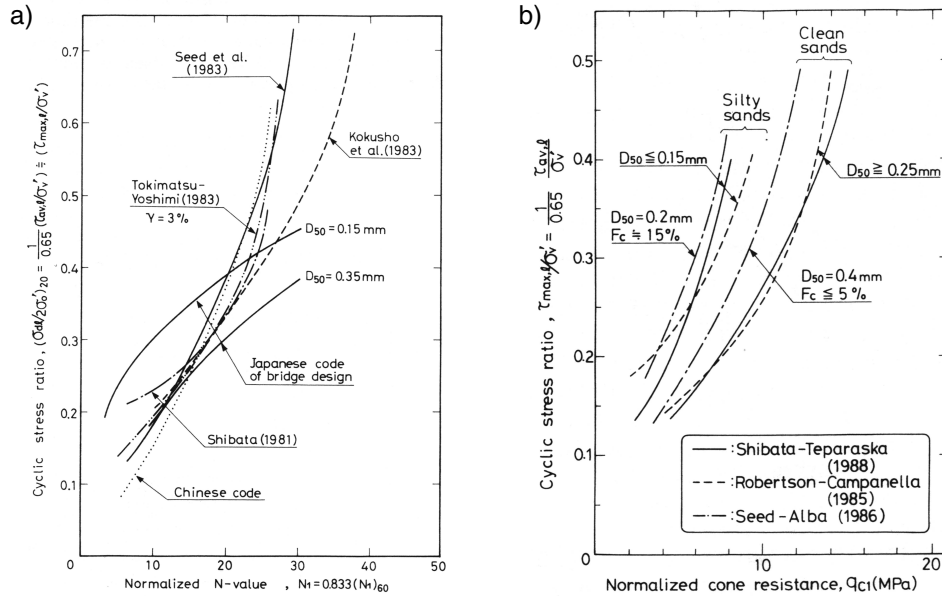


Fig. 3: Estimation of the liquefaction resistance from a) SPT and b) CPT data (Ishihara [14])

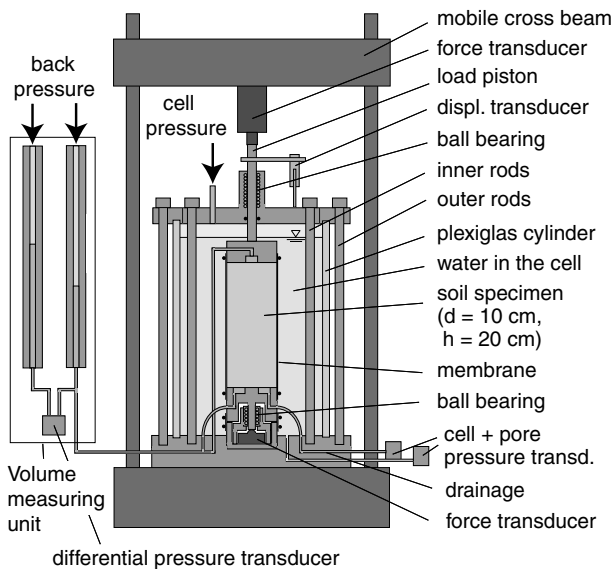


Fig. 4: Triaxial test device

pressure and back pressure were measured by means of pressure transducers.

Specimens were prepared by pluviating air-dry sand out of a funnel into a mould. After that they were fully saturated with de-aired water (Wichtmann et al. [4]). All tests were performed on a uniform medium coarse quartz sand (mean grain diameter $d_{50} = 0.55\text{ mm}$, uniformity index $U = d_{60}/d_{10} = 1.8$, $e_{min} = 0.577$, $e_{max} = 0.874$) with subangular grains, which was also used to develop the high-cycle accumulation model, Wichtmann et al. [2,3,4]. The grain size distribution

is given e.g. in [4].

In the following the total stress is $\sigma_i = \sigma'_i + u$ ($u =$ pore water pressure) and soil density is described by the density index $I_D = (e_{max} - e)/(e_{max} - e_{min})$.

4 Experimental results

The cyclic tests were preceded by undrained monotonous tests in order to determine the phase transformation (PT) and the failure lines (FL). Eight tests with triaxial compression and extension were performed with isotropic consolidation stresses $50\text{ kPa} \leq p_c = (\sigma'_{1c} + 2\sigma'_{3c})/3 \leq 200\text{ kPa}$ (the subscript c denotes "consolidation") and with an axial strain rate $|\dot{\epsilon}_1| = 0.05\text{ \%/min}$. The specimens had densities in the range $0.54 \leq I_D \leq 0.60$. The resulting stress paths in the p - q -plane and the failure lines are shown in Fig. 5.

In the cyclic tests specimens were prepared with initial densities $0.63 \leq I_{D0} \leq 0.68$. They were consolidated under isotropic conditions with $p_c = 100\text{ kPa}$. Thereafter, a drained cyclic preloading was applied stress-controlled. The axial stress σ_1 was cyclically varied with an amplitude $\sigma_{1,preload}^{ampl} = q_{preload}^{ampl}$ while the lateral stress σ_3 was maintained constant. Four cyclic histories with different amplitudes $q_{preload}^{ampl}$ and different numbers of cycles $N_{preload}$ were tried out, Table 1, where "cyclic preloading No. 1" means no cyclic preloading, i.e. the freshly pluviated sample. The stress amplitudes $q_{preload}^{ampl} = 30\text{ kPa}$ and $q_{preload}^{ampl} = 50\text{ kPa}$ correspond to shear strain amplitudes of $\gamma^{ampl} \approx 3.7 \cdot 10^{-4}$ and $\gamma^{ampl} \approx 7.0 \cdot 10^{-4}$, respectively.

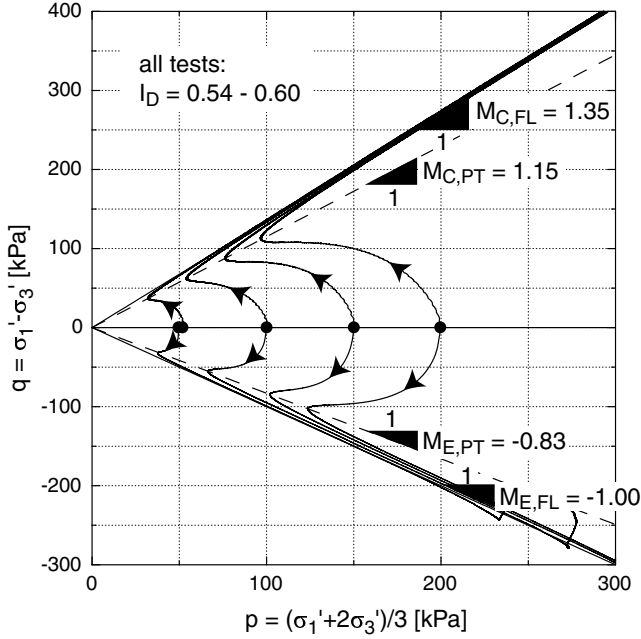


Fig. 5: Stress paths in the p - q -plane during monotonous undrained shear

Table 1: Tested cyclic preloadings

Cyclic preloading	$q_{\text{preload}}^{\text{ampl}}$ [kPa]	N_{preload} [-]
1	-	0
2	30	10
3	50	10
4	50	100

During the drained cyclic test phase the accumulation of strain was measured. Figure 6 presents typical curves of the volumetric ($\varepsilon_v = \varepsilon_1 + 2\varepsilon_3$) and the deviatoric ($\varepsilon_q = 2/3(\varepsilon_1 - \varepsilon_3)$) strain components with time during cyclic preloading. While the accumulation of deviatoric strain $\varepsilon_q^{\text{acc}}$ was negligible the residual volumetric strain $\varepsilon_v^{\text{acc}}$ increased with each load cycle. This approximately pure volumetric accumulation is typical for an isotropic average stress (see the "cyclic flow rule" presented by Wichtmann et al. [2]). Some of the volumetric average accumulation curves are shown in Fig. 7. For each cyclic preloading three curves $\varepsilon_v^{\text{acc}}(N)$ are presented. As expected the amplitude of 30 kPa causes less accumulation than 50 kPa (the accumulation rate is proportional to the square of the strain amplitude, Wichtmann et al. [2]).

After the application of the drained cyclic preloading the drainage of the triaxial device was closed and the undrained cyclic test phase was started. The total axial stress σ_1 was oscillated with an amplitude

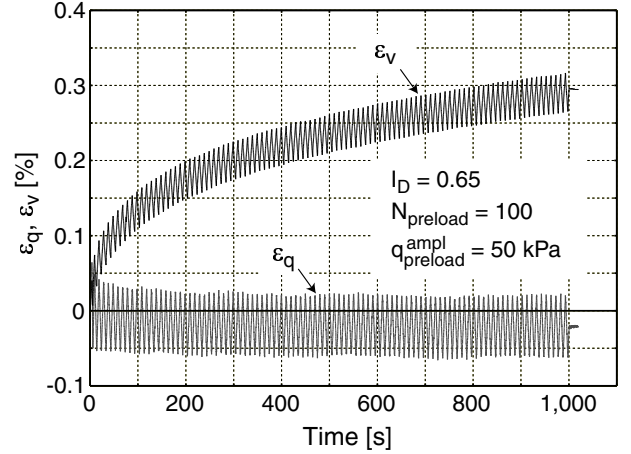


Fig. 6: Accumulation of volumetric (ε_v) and deviatoric (ε_q) strain during drained cyclic preloading

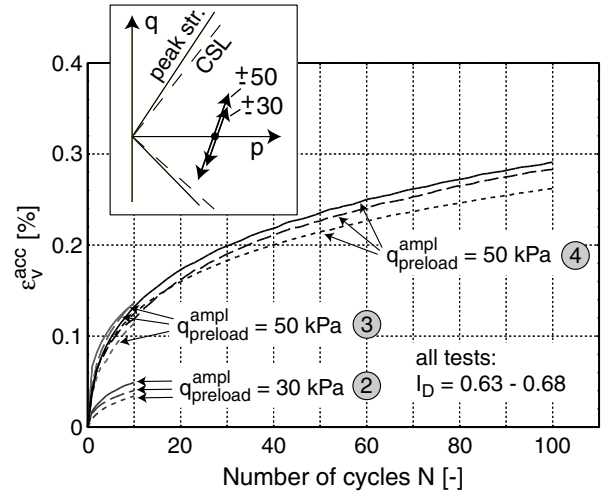


Fig. 7: Average accumulation curves $\varepsilon_v^{\text{acc}}(N)$ during drained cyclic preloading (the numbers in the gray circles correspond to Table 1)

$\sigma_1^{\text{ampl}} = q^{\text{ampl}}$ while the total lateral stress σ_3 was kept constant. For each of the four cyclic preloadings several tests with varying amplitudes q^{ampl} during the undrained phase were performed.

Figure 8 presents the increase of the pore water pressure u during undrained cyclic loading in four tests with different cyclic preloadings but an identical amplitude $q^{\text{ampl}} = 45$ kPa in the undrained phase. If the pore water pressure reached the total lateral stress σ_3 the specimen had undergone "initial liquefaction" accompanied by the well known cyclic mobility phenomenon. An increase of the intensity of drained cyclic preloading (in the amplitude and/or in the number of cycles) reduces the rate of pore pressure accumulation $\dot{u} = \partial u / \partial N$ and it therefore takes more cycles to reach initial liquefaction. The fresh (non-preloaded) specimens needed about 5 cycles to initial liquefaction compared to 8 cy-

cles in the case of the specimen preloaded with $q_{\text{preload}}^{\text{ampl}} = 30$ kPa and $N_{\text{preload}} = 10$. The preloading with $q_{\text{preload}}^{\text{ampl}} = 50$ kPa and $N_{\text{preload}} = 10$ delayed the initial of liquefaction to occur after 43 cycles and 205 cycles were needed for the specimen preloaded with $q_{\text{preload}}^{\text{ampl}} = 50$ kPa and $N_{\text{preload}} = 100$.

While the amplitude of the vertical strain $\varepsilon_1^{\text{ampl}}$ was small during the first cycles it increased strongly during the cycle that lead to initial liquefaction (Fig. 9) and grew with each subsequent cycle. The generated strain amplitudes were nearly symmetric in triaxial extension and compression. From Fig. 9 it is obvious, that independent of the cyclic preloading full liquefaction (defined as the time when a double amplitude of vertical strain $2\varepsilon_1^{\text{ampl}} = 10\%$ was reached) and the failure of the sample occurred within four or five cycles after initial liquefaction. In each test failure occurred in the extension regime of the p - q -plane.

Figure 10 presents the stress-strain hysteresis and the stress paths in the p - q -plane are shown in Fig. 11. There is no principal difference in the shape of the hysteresis or the run of the stress paths for the different cyclic preloadings except that the number of cycles to liquefaction increases with the intensity of cyclic preloading.

In Fig. 12 for each test the cyclic stress ratio $CSR = q^{\text{ampl}}/(2p_c)$ is plotted versus the cycle number N that was necessary to generate a double amplitude $2\varepsilon_1^{\text{ampl}} = 10\%$. For a given cyclic preloading it is obvious that higher stress amplitudes q^{ampl} in the undrained test phase caused an earlier liquefaction. Due to cyclic preloading the curves $CSR(N)$ are shifted upwards in Fig. 12. It is therefore obvious that a cyclic preloading may considerably increase the cyclic undrained strength. For the non-preloaded specimen full liquefaction in 15 cycles is reached with a stress ratio $CSR_{N=15} = 0.189$. For cyclic preloadings No. 2, 3 and 4 this value is $CSR_{N=15} = 0.208$, $CSR_{N=15} = 0.259$ and $CSR_{N=15} = 0.295$, respectively.

In drained cyclic triaxial tests (Wichtmann et al. [4]) the rate of total strain accumulation $\dot{\varepsilon}^{\text{acc}} = \partial\varepsilon^{\text{acc}}/\partial N$ (with $\dot{\varepsilon} = \sqrt{(\dot{\varepsilon}_1)^2 + 2(\dot{\varepsilon}_3)^2}$) was found proportional to the square of the total strain amplitude $\varepsilon^{\text{ampl}}$. In the accumulation model (Niemunis et al. [1]) this is captured by the function

$$f_{\text{ampl}} = (\varepsilon^{\text{ampl}}/\varepsilon_{\text{ref}}^{\text{ampl}})^2 \quad (1)$$

with the reference amplitude $\varepsilon_{\text{ref}}^{\text{ampl}} = 10^{-4}$. The residual strain rate decreases with N according to

$$\dot{\varepsilon}^{\text{acc}} \sim \dot{f}_N = \frac{C_{N1}C_{N2}}{1 + C_{N2}N} + C_{N1}C_{N3} \quad (2)$$

The material constants are $C_{N1} = 3.4 \cdot 10^{-4}$, $C_{N2} = 0.55$ and $C_{N3} = 6.0 \cdot 10^{-5}$ for the tested sand (Wicht-

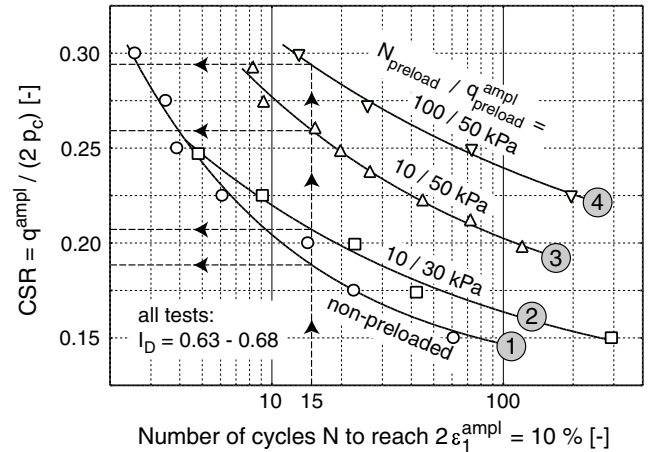


Fig. 12: Relationship between the cyclic stress ratio $CSR = q^{\text{ampl}}/(2p_c)$ and the number of cycles N to cause a double amplitude $2\varepsilon_1^{\text{ampl}} = 10\%$ for different cyclic preloadings

mann et al. [4]). The first term of the rate \dot{f}_N is dependent on the number of cycles. A state variable for cyclic preloading should consider the number of cycles and their amplitude. For this purpose the state variable g^A has been defined (Niemunis et al. [1]). It weights the number of preloading cycles with their total strain amplitudes $\varepsilon^{\text{ampl}}$:

$$g^A = \int f_{\text{ampl}} \frac{C_{N1}C_{N2}}{1 + C_{N2}N} dN \quad (3)$$

For $\varepsilon^{\text{ampl}} = \text{constant}$ Eq. (3) simplifies to

$$g^A = f_{\text{ampl}} C_{N1} \ln(1 + C_{N2}N) \quad (4)$$

The state variable g^A was calculated for the four cyclic preloadings and in Fig. 13 the cyclic stress ratio causing liquefaction in 15 cycles $CSR_{N=15}$ is plotted versus g^A . $CSR_{N=15}$ increases with g^A according to

$$\begin{aligned} CSR_{N=15} &= CSR_{N=15,0} f(g^A) \quad \text{with} \\ f(g^A) &= 1 + C_{g1} \ln(1 + C_{g2} g^A) \end{aligned} \quad (5)$$

with the material constants $C_{g1} = 0.46$ and $C_{g2} = 51.6$. $CSR_{N=15,0} = 0.189$ is the cyclic stress ratio for the reference state $g^A = 0$ (non-preloaded soil) and a void ratio $e_{\text{ref}} = 0.681$ ($I_D = 0.65$).

5 Prospective application of the correlation

Having performed SPT or CPT soundings in situ, a profile with depth of $CSR_{N=15}$ can be obtained from threshold curves as those in Figs. 2 and 3. An example of a profile of $CSR_{N=15}$ with depth z (after Robertson and Campanella [35]) is shown in Fig. 14.

If correlation diagrams as those in Figs. 2 and 3 are unavailable (e.g. in regions with little seismic activity)

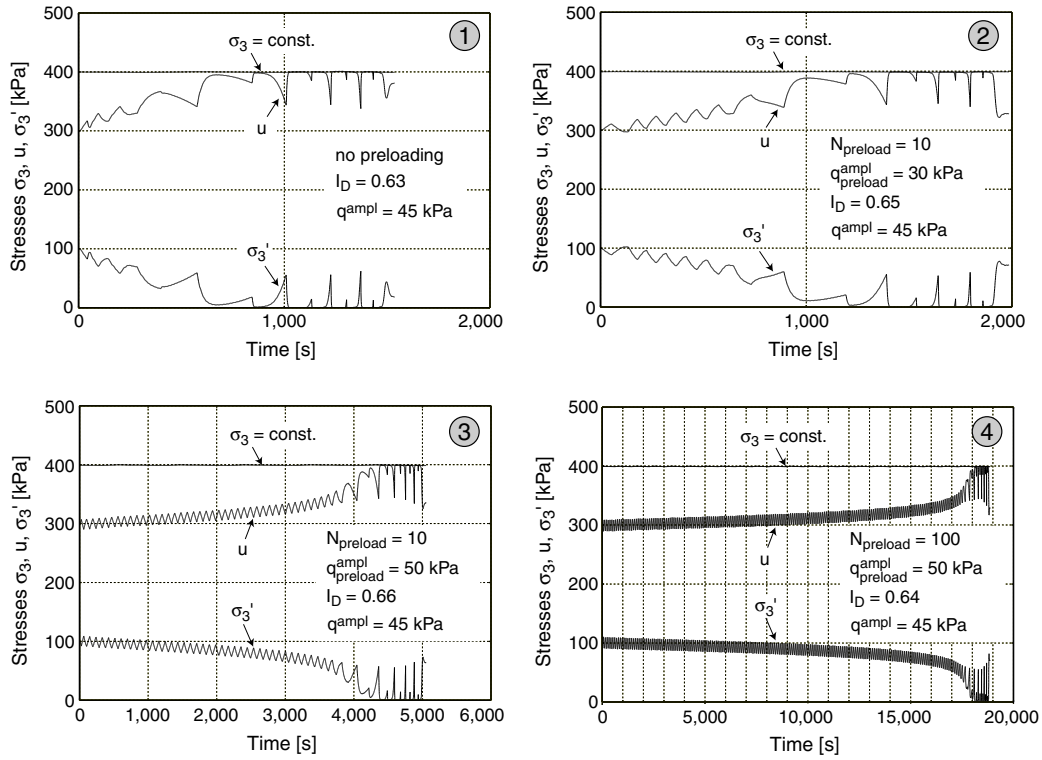


Fig. 8: Development of the pore pressure u and effective lateral stress σ_3' during undrained cyclic loading in four tests on specimens with varying cyclic preloading (all tests: $q^{ampl} = 45$ kPa)

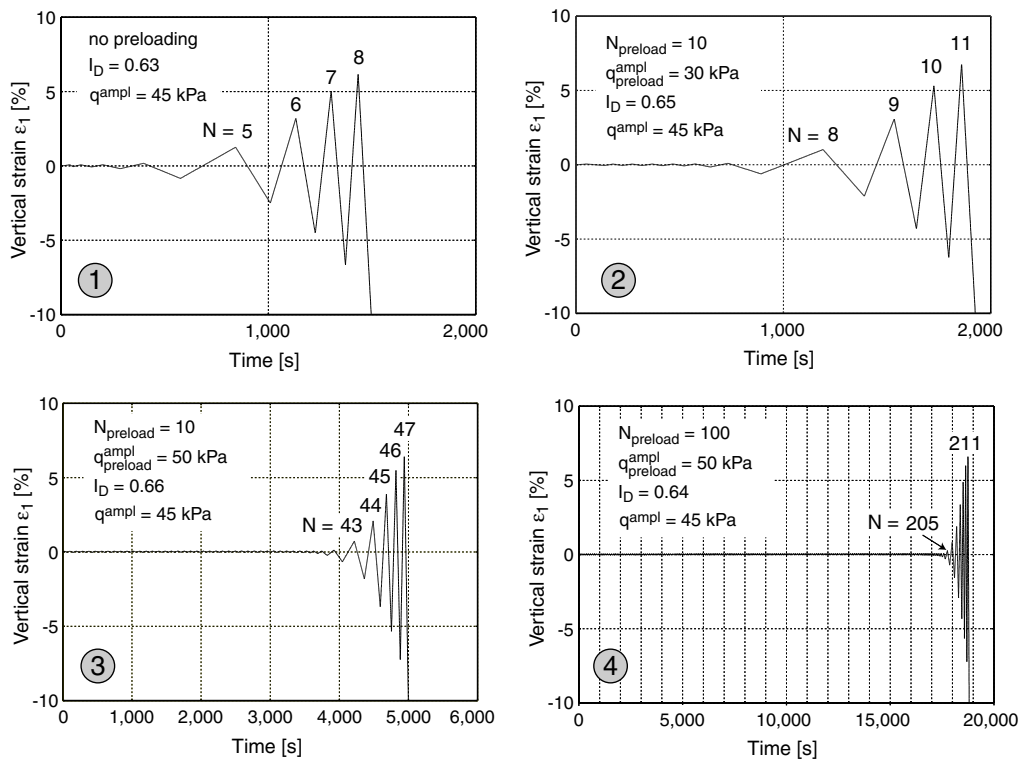


Fig. 9: Development of the vertical strain ϵ_1 during undrained cyclic loading in four tests on specimens with varying cyclic preloading (all tests: $q^{ampl} = 45$ kPa)

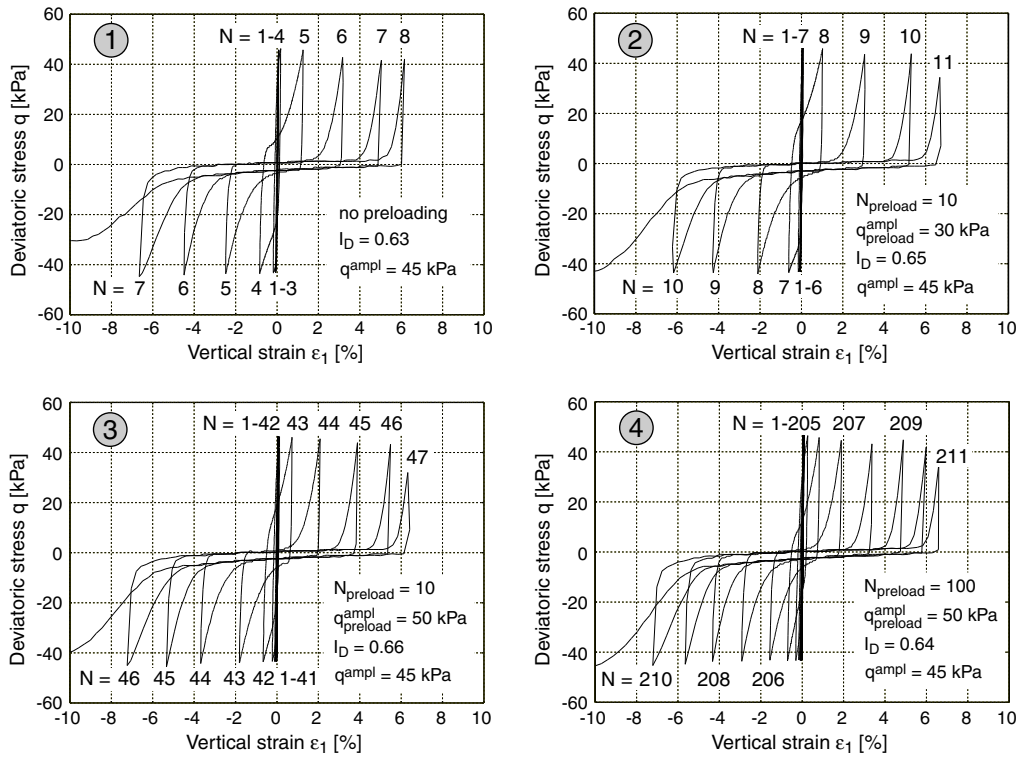


Fig. 10: Stress-strain hysteresis for different cycle numbers N during undrained cyclic loading in four tests on specimens with varying cyclic preloading (all tests: $q^{ampl} = 45$ kPa)

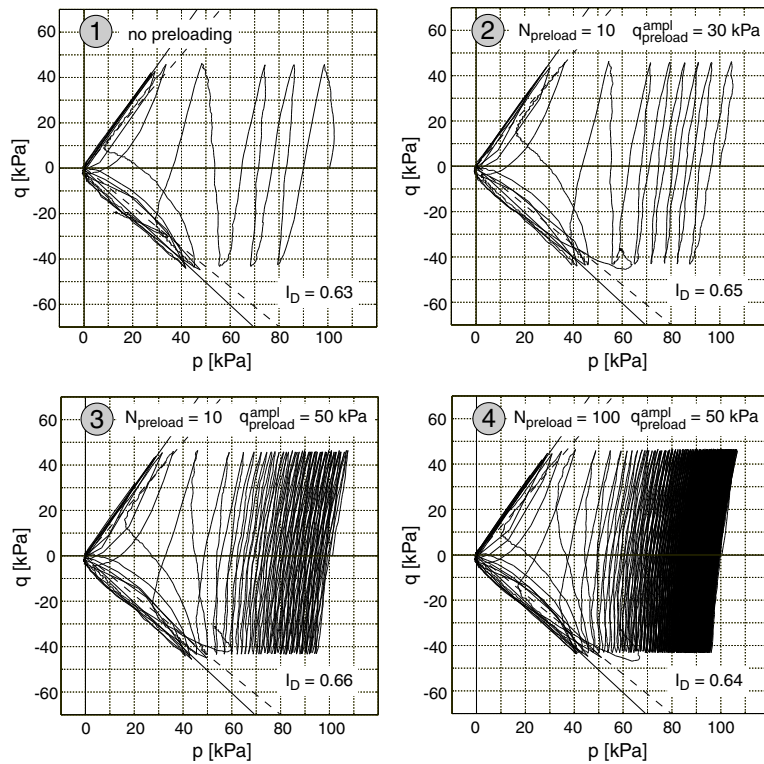


Fig. 11: Stress paths in the p - q -plane during undrained cyclic loading in four tests on specimens with varying cyclic preloading (all tests: $q^{ampl} = 45$ kPa)

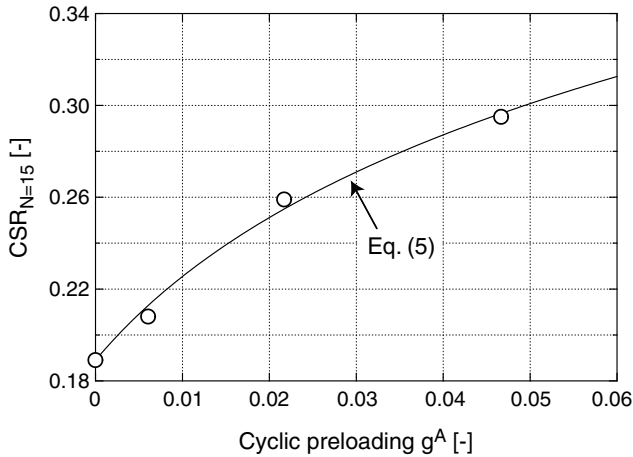


Fig. 13: Cyclic undrained strength $CSR_{N=15}$ in dependence of cyclic preloading g^A

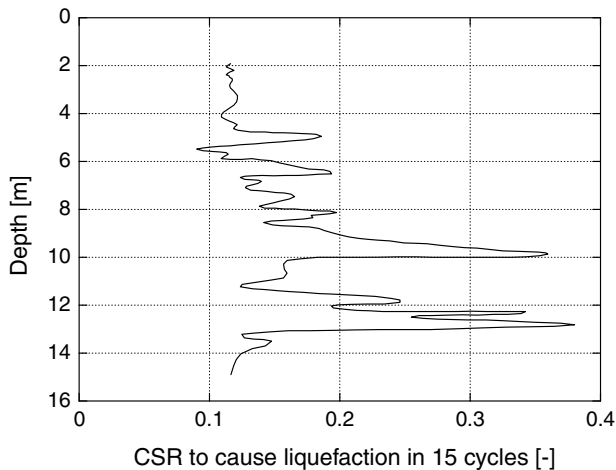


Fig. 14: Example of a profile $CSR_{N=15}(z)$ after Robertson and Campanella [35]

a curve from the literature has to be chosen based on similar grain characteristics and fines content. Unfortunately, there is some scatter between the curves of several researchers or codes of practice.

From a few tests performed on re-constituted disturbed specimens a curve $CSR(N)$ similar to curve No. 1 in Fig. 12 corresponding to the non-preloaded specimens is established and $CSR_{N=15,0}$ is determined. The tests should be performed with the in-situ density. However, if this density varies strongly it may be more appropriate to determine $CSR_{N=15,0}$ for a constant void ratio e_{ref} and to introduce a void ratio correction function $f(e)$ with $f(e) = 1$ for $e = e_{ref}$. The function $f(e) = 1 + e_{ref} - e$ would be suitable for the data presented by Seed and Lee [42], Fig. 15. Assuming Eq. (5) to be valid independent of the fines content and the grain size distribution (which has to be checked in future) cyclic preloading g^A for a certain depth can be

obtained from

$$CSR_{N=15} = CSR_{N=15,0} f(g^A) f(e) \quad (6)$$

Note that Eq. (6) neglects the influence of stress on the liquefaction resistance (similarly as Seed and Lee [42] do). The SPT blow number and the CPT tip resistance are increased also by aging. Following the above procedure aging effects are equivalent to cyclic preloading. This is in accordance with experiments of Seed [12], which show a decrease of the cyclic accumulation rate due to aging.

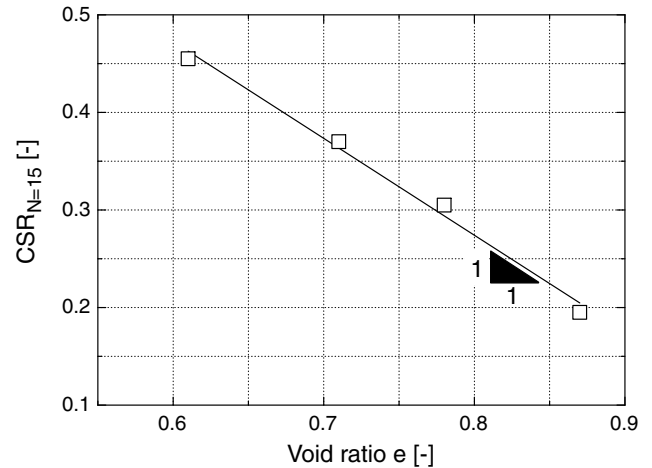


Fig. 15: $CSR_{N=15}$ as a function of void ratio after Seed and Lee [42]

6 Summary and conclusions

Our aim is the prediction of residual settlements in a non-cohesive soil under cyclic loading with many ($N > 10^3$) small ($\varepsilon^{amp1} \leq 10^{-3}$) cycles. Beside stress and void ratio the accumulation rate is significantly influenced by cyclic preloading. Since the cyclic preloading of an in-situ soil cannot be measured directly, it has to be determined from simple correlations. In order to study a correlation of cyclic preloading with the liquefaction resistance undrained cyclic triaxial tests were performed on specimens which were subject to a drained cyclic preloading. These tests reveal a strong correlation between cyclic preloading and the liquefaction resistance. A prospective application of the correlation using SPT or CPT data was proposed.

Acknowledgements

This study was conducted as a part of the project A8 "Influence of the fabric change in soil on the lifetime of structures", supported by the German Research Council (DFG) within the Centre of Excellence SFB 398 "Lifetime oriented design concepts". The authors are grateful to DFG for the financial support.

References

- [1] Niemunis A, Wichtmann T, Triantafyllidis T. A high-cycle accumulation model for sand. *Computers and Geotechnics* (in print).
- [2] Wichtmann T, Niemunis A, Triantafyllidis T. Strain accumulation in sand due to drained uniaxial cyclic loading. In Triantafyllidis (ed.) *Cyclic Behaviour of Soils and Liquefaction Phenomena*, Proc. of CBS04, Bochum, 2004:233-46. Balkema.
- [3] Wichtmann T, Niemunis A, Triantafyllidis T. The effect of volumetric and out-of-phase cyclic loading on strain accumulation under cyclic loading. In Triantafyllidis (ed.) *Cyclic Behaviour of Soils and Liquefaction Phenomena*, Proc. of CBS04, Bochum, 2004:247-56. Balkema.
- [4] Wichtmann T, Niemunis A, Triantafyllidis T. Strain accumulation in sand due to cyclic loading: drained triaxial tests. *Soil Dynamics and Earthquake Engineering* (in print).
- [5] Yoshimi Y, Hatanaka M, Oh-Oka H. Undisturbed sampling of saturated sands by freezing. *Soils Foundations* 1978;18(3):105-11.
- [6] Hofmann BA. In-situ ground freezing to obtain undisturbed samples of loose sand for liquefaction assessment. PhD thesis. University of Alberta, Edmonton; 1997.
- [7] Humme B. Struktur von granularen Medien und deren Änderung infolge zyklischer Belastung. Diploma thesis. Institute of Foundation Engineering and Soil Mechanics, Ruhr-University Bochum; 1999.
- [8] Niemunis A. Extended hypoplastic models for soils. *Habilitation*. Institute of Foundation Engineering and Soil Mechanics, Ruhr-University Bochum, Issue No. 34; 2003.
- [9] Wichtmann T, Triantafyllidis Th. Influence of a cyclic and dynamic loading history on dynamic properties of dry sand, part I: cyclic and dynamic torsional prestraining. *Soil Dynamics and Earthquake Engineering* 2004;24(2):127-47.
- [10] Wichtmann T, Triantafyllidis Th. Influence of a cyclic and dynamic loading history on dynamic properties of dry sand, part II: cyclic axial preloading. *Soil Dynamics and Earthquake Engineering* 2004;24(11):789-803.
- [11] Yoshimi Y, Richart FE, Prakash S, Balkan DD, Ilyichev YL. Soil dynamics and its application to foundation engineering. In: *Proceedings of the 9th International Conference on Soil Mechanics and Foundation Engineering*, Tokyo; 2:605-50.
- [12] Seed HB. Soil liquefaction and cyclic mobility evaluation for level ground during earthquakes. *J Geotech Engng Div, ASCE* 1979;105(GT2):201-55.
- [13] Dobry R, Ladd RS, Yokel FY, Chung RM, Powell D. Prediction of pore pressure buildup and liquefaction of sands during earthquakes by the cyclic strain method. Report No. 138, U.S. Department of Commerce, National bureau of standards, NBS Building science series; 1982.
- [14] Ishihara K. Liquefaction and flow failure during earthquakes. The 33rd Rankine Lecture. *Géotechnique* 1993;43(3):351-415.
- [15] Robertson PK, Fear CE. Liquefaction of sands and its evaluation. Keynote Lecture. In: *IS Tokyo'95, Proceedings of the 1st International Conference on Earthquake Geotechnical Engineering*, 1995.
- [16] Triantafyllidis Th (ed). *Cyclic Behaviour of Soils and Liquefaction Phenomena*, Proc. of CBS04, Bochum, March/April 2004. Balkema.
- [17] Nemat-Nasser S, Takahashi K. Liquefaction and densification of sand. *J Geotech Engng, ASCE* 1984;110(9):1291-306.
- [18] Ladd RS. Specimen preparation and liquefaction of sands. *J Geotech Engng Div, ASCE* 1974;100(GT10):1180-84.
- [19] Mulilis JP, Chan CK, Seed HB. The effects of method of sample preparation on the cyclic stress-strain behavior of sands. Report No. EERC 75-18, Earthquake Engineering Research Center, University of California, Berkeley, 1975.
- [20] Mulilis JP, Seed HB, Chan CK, Mitchell JK, Arulanandan K. Effects of sample preparation on sand liquefaction. *J Geotech Engng Div, ASCE* 1977;103(GT2):91-108.
- [21] Porcino D, Ciccù G, Ghionna VN. Laboratory investigation of the undrained cyclic behaviour of a natural coarse sand from undisturbed and reconstituted samples. In Triantafyllidis (ed.) *Cyclic Behaviour of Soils and Liquefaction Phenomena*, Proc. of CBS04, Bochum, 2004:187-92. Balkema.
- [22] Oda M, Kawamoto K, Suzuki K, Fujimori H, Sato M. Microstructural interpretation on reliquefaction of saturated granular soils under cyclic loading. *J Geotech Geoenviron Engng, ASCE* 2001;127(5):416-23.
- [23] Tokimatsu K, Hosaka Y. Effects of sample disturbance on dynamic properties of sand. *Soils Foundations* 1986;26(1):53-64.
- [24] Hatanaka M, Suzuki Y, Kawasaki T, Endo M. Cyclic undrained shear properties of high quality undisturbed Tokyo gravel. *Soils Foundations* 1988;28(4):57-68.
- [25] Finn WDL, Bransby PL, Pickering DJ. Effect of strain history on liquefaction of sand. *J Soil Mech Foundations Div, ASCE* 1970;96(SM6):1917-34.
- [26] Seed HB, Mori K, Chan CK. Influence of seismic history on liquefaction of sands. *J Geotech Engng Div* 1977;103(GT4):257-70.
- [27] Seed RB, Lee SR, Jong HL. Penetration and liquefaction resistances: prior seismic history effects. *J Geotech Engng* 1988;114(6):691-97.
- [28] Teachavoransinsun S, Tatsuoka F, Lo Presti DCF. Effects of cyclic prestraining on dilatancy characteristics and liquefaction of sand. In Shibuya, Mitachi, Miura (eds) *Pre-failure deformation of geomaterials* 1994:75-80.
- [29] Ishihara K, Okada S. Effects of stress history on cyclic behavior of sands. *Soils Foundations* 1978;18(4):31-45.

[30] Ishihara K, Okada S. Effects of large preshearing on cyclic behavior of sand. *Soils Foundations* 1982;22(3):109-25.

[31] Suzuki T, Toki S. Effects of preshearing of liquefaction characteristics of saturated sand subjected to cyclic loading. *Soils Foundations* 1984;24(2):16-28.

[32] Emery JJ, Finn WDL, Lee KW. Uniformity of saturated sand specimen. ASTM, Report No. STP523, 1973:182-94.

[33] Seed HB, Idriss IM. Simplified procedure for evaluating soil liquefaction potential. *J Soil Mech Foundations Div* 1971;97(SM9):1249-73.

[34] Seed HB, Arango I, Chan CK. Evaluation of soil liquefaction potential during earthquakes. Report No. EERC 75-28, Earthquake Engineering Research Center, University of California, 1975.

[35] Robertson PK, Campanella RG. Liquefaction potential of sands using the cone penetration test. *J Geotech Engng* 1985;22(3):298-307.

[36] Seed HB, de Alba P. Use of SPT and CPT tests for evaluating the liquefaction resistance of sands. In Clemence SP (ed) *Use of in situ tests in geotechnical engineering*, Geotechnical Special Publication, ASCE 1986;6:281-302.

[37] Mitchell JK, Tseng DJ. Assessment of liquefaction potential by cone penetration resistance. In Duncan JM (ed) *Proc. of the H. Bolton Seed Memorial Symposium*, Berkeley, California 1990;2:335-50. Bitech Publishers.

[38] Olsen RS, Koester JP. Prediction of liquefaction resistance using the CPT. In: *Proc. of the International Symposium on Cone Penetration Testing, CPT'95*, Linkoping, Sweden 1995;2:251-56.

[39] Suzuki Y, Tokimatsu K, Koyamada K, Taya Y, Kubota Y. Field correlation of soil liquefaction based on CPT data. In: *Proc. of the International Symposium on Cone Penetration Testing, CPT'95*, Linkoping, Sweden 1995;2:583-88.

[40] Stark TD, Olson SM. Liquefaction resistance using CPT and field case histories. *J Geotech Engng* 1995;121(12):856-69.

[41] Robertson PK, Wride CE. Evaluating cyclic liquefaction potential using the cone penetration test. *Can Geotech J* 1998;35:442-59.

[42] Seed HB, Lee KL. Studies of liquefaction of sands under cyclic loading conditions. Report No. TE-65-65, Dept. of Civil Engineering, University of California, Berkeley, 1965.